The Dimer of Acetylene and the Dimer of Diacetylene: A Floppy and a Very Floppy Molecule

Alfred Karpfen*

Institut für Theoretische Chemie und Strahlenchemie der Universität Wien, A-1090 Wien, Währingerstrasse 17, Austria

Received: July 27, 1999; In Final Form: October 19, 1999

The intermolecular energy surfaces of the acetylene dimer and of the diacetylene dimer were investigated at the Møller−Plesset second order level applying medium to large basis sets. For both dimers extensive 2D scans of selected sections of the energy surfaces were carried out. In agreement with previous experimental and theoretical studies, there is only one energy minimum on the intermolecular energy surface of the acetylene dimer; a C_{2v} π-type hydrogen-bonded structure. Apart from the C_{2h} slipped parallel first-order saddle point, a weakly bound second-order saddle point of D_{2d} symmetry was detected as well. A topologically much richer situation has been encountered in the case of the diacetylene dimer, for which neither experimental nor theoretical studies had been available so far. Four energy minima were detected. The most stable configuration is a C_{2h} slipped parallel structure. Two minima are energetically very close-lying: a tilted C_s hydrogen-bonded conformation and an orthogonal D_{2d} arrangement. The fourth minimum is a further, somewhat higher-lying C_{2h} slipped parallel structure. All minima and a few high-symmetry saddle points were characterized with the aid of vibrational analysis.

Introduction

The gas-phase intermolecular interaction between nonpolar molecules containing conjugated triple bonds has rarely been probed from the experimental side nor has it been investigated with high-level ab initio methods. In contrast, for the dimer of acetylene a great deal of systematic work has already been done. The structure, dynamics, and the relevant sections of the energy surface of the acetylene dimer have already been studied extensively by microwave and infrared spectroscopic investigations[1−5] and by various theoretical methods.[6−14] However, for the next member of the polyyne series, diacetylene (1,3-butadiyne), no experimental data on the spectroscopy of the vapor phase dimer has been reported so far. From the theoretical side, only a single density functional study of a spatially very restricted region of the diacetylene dimer was recently presented.[15]

In a series of systematic theoretical investigations on the intermolecular interaction of the homodimers of the smaller members of the cyanopolyyne family performed by this author (hydrogen cyanide dimer,[16] cyanoacetylene dimer,[16,17] and the dimer of cyanodiacetylene[18]), the importance of stacked, non-hydrogen-bonded configurations has been evaluated in addition to that of the linear structures with C−H···N≡C hydrogen bonds. The main trend in the cyanopolyyne homodimer series extracted from these investigations[18] is that with increasing chain length of the cyanopolyyne, the stacked non-hydrogen-bonded structures tend to become significantly more stable than the linear hydrogen-bonded dimers. The turning point in this series is the dimer of cyanodiacetylene for which the stacked structure is already distinctly more stable, whereas in the case of the cyanoacetylene dimer the linear hydrogen-bonded configuration is just a trifle more stable than the stacked configuration; the latter is not a minimum but a first-order saddle point in the case of the hydrogen cyanide dimer. This behavior is merely a consequence of the increasing importance of dispersion contributions to the intermolecular interaction energy with increasing chain length of the cyanopolyyne.

In this work, the energy surface of the diacetylene dimer was investigated in some detail. To walk on safe grounds and for the purpose of comparison, the dimer of acetylene was also studied at the very same and certain aspects also at higher levels of sophistication. It is quite well established that the most stable structure of the acetylene dimer is a π-type hydrogen-bonded arrangement with C_{2v} symmetry. The slipped parallel or stacked structure with C_{2h} symmetry is a first-order saddle point, energetically only slightly above the C_{2v} minimum. As elucidated by microwave studies,[3−5] the major dynamical pathway of the acetylene dimer may be viewed as a *geared* rotation of the two molecules with C_{2h} saddle points between energetically equivalent C_{2v} minima. Throughout this minimum energy path the acetylene dimer prefers planar structures.

Quite in analogy to the cyanopolyyne series, a richer-structured energy surface with different types of minima can be expected for the diacetylene dimer. In addition to the π-type hydrogen-bonded arrangement, slipped parallel or stacked structures might also be promising candidates. Nonplanar structures which do not play a significant role for the dynamics of the acetylene dimer could, however, be important in the case of the diacetylene dimer. Since this is the first systematic investigation on the intermolecular energy surface of the diacetylene dimer, emphasis was laid (i) on a qualitative understanding of the energy surface, thereby testing the methodical and basis set requirements for a proper description of the system, (ii) on the characterization of the minima including the prediction of spectroscopically observable features, such as vibrational frequency shifts, and (iii) on a detailed comparison to the better understood case of the acetylene dimer

* Corresponding author. Phone: (+43-1) 4277-52760. Fax: (+43−1) 4277−9527. E-mail: Alfred.Karpfen@univie.ac.at.

10.1021/jp992605r CCC: $18.00
Published on Web 11/25/1999

TABLE 1: Computed Total Energies (E), Optimized Bond Distances, Rotational Constants (B_e), Quadrupole Moments (Θ), and Parallel ($\alpha_{||}$) and Perpendicular ($\alpha_{\perp}$) Polarizabilities of the Acetylene Monomer

basis set	method	E [hartree]	r(H−C) [Å]	r(C≡C) [Å]	B_e [GHz]	Θ [debye Å]	$\alpha_{||}$ [Å^3]	$\alpha_{\perp}$ [Å^3]
I	MP2	−77.11766	1.0617	1.2068	35.27	6.30	4.34	1.66
II	MP2	−77.14146	1.0637	1.2104	35.08	6.67	4.44	2.20
III	MP2	−77.14266	1.0639	1.2109	35.06	6.56	4.54	2.79
III	MP2(full)	−77.20224	1.0630	1.2091	35.15	6.54	4.53	2.78
III	RHF	−76.85148	1.0547	1.1799	36.61	7.09	4.49	2.78
III	B3LYP	−77.33954	1.0626	1.1963	35.73	6.58	4.67	2.89
IV[e]	MP2	−77.13358	1.0617	1.2107	35.10	6.55	4.52	2.66
V[f]	MP2	−77.08268	1.0755	1.2298	34.07	6.42	4.23	1.38
VI[g]	MP2	−77.15920	1.0613	1.2114	35.08	6.51	4.33	2.02
VII[h]	MP2	−77.09300	1.0752	1.2315	34.00	6.76	4.69	2.75
VIII[i]	MP2	−77.16410	1.0615	1.2122	35.04	6.57	4.54	2.80
experiment			1.0621[a]	1.2026[a]	35.45	7.61[b]	4.68[c]	2.89[c]
						6.15[c]	4.53[d]	2.78[d]

[a] Data from ref 41. [b] Data from ref 42. [c] Data from ref 43. [d] Data from ref 44. [e] 6-311++G(3df,3pd). [f] cc-pVDZ. [g] cc-pVTZ. [h] aug-cc-pVDZ. [i] aug-cc-pVTZ.

which, quite apart from a discussion of the different structural features, allows also to assess eventual shortcomings of the current calculations due to unavoidable compromises in the choice of the basis set and in the treatment of electron correlation. It was not the aim of the current study to compute sufficient points to allow for the development of analytical 4D energy surfaces for the two dimers.

Method of Calculation

In this work, all quantum chemical calculations were performed with the Gaussian 94[19] and Gaussian 98[20] suites of programs. For most of the calculations the standard Møller−Plesset second-order (MP2)[21] approach was used. This choice is dictated by the need to use a method that includes the contribution of the dispersion interaction to the intermolecular interaction energy at a sufficiently reliable level. MP2 fulfills this criterion. Only the valence electrons were correlated. The effects of going beyond MP2 and of correlating the core electrons as well are illustrated at the stationary points found for the acetylene dimer. Improvements up to MP4(SDTQ)[22] and CCSD(T)[23−27] were evaluated for the interaction energies using MP2 optimized structures. In general, ab initio self-consistent field (SCF) and density functional methods are not applicable in cases where the electrostatic contribution to the intermolecular interaction is not the by far dominating term. Nevertheless, examples are shown in the acetylene dimer case using SCF and B3LYP approaches.[28−31]

Guided by the experience gained from our previous investigations on the intermolecular interaction of cyanopolyynes,[16−18] the same basis sets were also applied in this work. Basis set I is the 10s6p/6s basis set of Huzinaga[32,33] contracted to 6s4p/4s and augmented by a set d functions on carbon (1.0) and a set of p functions on hydrogen (0.75). Basis set II is the 11s7p/6s Huzinaga basis set[32,33] augmented by two sets of d functions on carbon (1.0, 0.3) and a set of p functions on hydrogen (0.75). Basis set III consists of basis set II plus additional flat s, p, and d functions on carbon (0.03/0.02/0.1) and flat s and two sets of p functions on hydrogen (0.03/0.2,0.05), thus overall a contracted 8s6p3d/7s3p basis. Basis sets I−III of this work correspond to basis sets II−IV of refs 17 and 18. In addition to these basis sets, which were used for both dimers, other large basis sets such as 6-311++G(3df,3dp) (IV) basis[34−36] and several of Dunning's correlation-consistent basis sets[37−39] with and without diffuse functions (cc-pVDZ, cc-PVTZ, aug-cc-pVDZ, aug-cc-PVTZ; (V−VIII)) were used for the acetylene and diacetylene monomers and for the acetylene dimer as well.

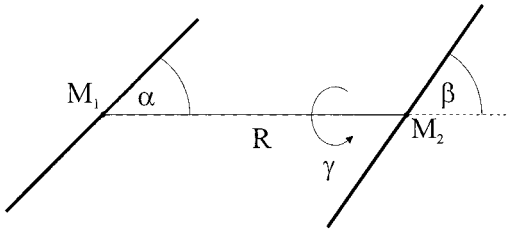

Figure 1. Schematic drawing of the coordinate system to describe the 4D intermolecular energy surface of the acetylene dimer and the diacetylene dimer. R is the distance between the two centers of mass M_1 and M_2. α and β are the two angles between the molecules' axes and the line connecting the centers of mass. γ is the torsional angle.

At all minima detected and at a few high-symmetry stationary points, full geometry optimizations were carried out. Harmonic vibrational frequencies were also calculated. The resulting stabilization energies were then corrected for zero point energy (ZPE) effects and for the basis set superposition error (BSSE)[40] including the influence of geometry relaxation in the complexes.

The 2D scans of the MP2 energy surfaces of the two dimers were calculated mostly with basis sets I and II without correcting for BSSE effects. That suffices to get an overview of the surface topology; moreover, correcting the basis set I calculations for BSSE does not improve, but rather worsens the results. In a few cases, basis set III has been used too. The monomer structures were kept frozen at the respective monomer equilibrium geometries. The coordinate system chosen for these scans is sketched in Figure 1.

Results and Discussion

A. The Monomers. *Acetylene.* The calculated total energies, the optimized bond distances, the rotational constants, the quadrupole moments, the polarizabilities parallel and perpendicular to the molecular axis, and the harmonic vibrational frequencies of the acetylene monomer as obtained at the MP2 level using different basis sets are compiled in Tables 1 and 2. For the purpose of evaluation, the best available experimental data are included as well in both tables. Comparison may also be made to similar extended compilations of ab initio results[47−50] on the acetylene monomer. These detailed comparisons are necessary since it is evident that all errors present in the description of the monomers will be carried over to the dimers as well.

The computed structural parameters (bond distances and rotational constants), the calculated quadrupole moment, and the polarizability in the direction of the long molecular axis,

TABLE 2: Computed Harmonic Vibrational Frequencies of the Acetylene Monomer[a]

basis set	method	ω_1 (σ_g^+)	ω_2 (σ_g^+)	ω_3 (σ_u^-)	ω_4 (π_g)	ω_5 (π_u)
I	MP2	3556	1992	3468	523	733
II	MP2	3519	1976	3430	550	716
III	MP2	3515	1971	3427	491	709
III	MP2(full)	3521	1977	3432	507	710
III	RHF	3663	2212	3552	788	852
III	B3LYP	3507	2066	3407	642	753
IV[b]	MP2	3525	1969	3431	533	737
V[c]	MP2	3540	1965	3456	558	749
VI[d]	MP2	3543	1975	3449	587	751
VII[e]	MP2	3519	1946	3432	408	703
VIII[f]	MP2	3536	1968	3434	600	752
experiment[g]		3495	2008	3415	624	747
experiment[h]		3374	1974	3289	612	730

[a] All values in cm^{-1}. [b] 6-311++G(3df,3pd). [c] cc-pVDZ. [d] cc-pVTZ. [e] aug-cc-pVDZ. [f] aug-cc-pVTZ. [g] Experimental harmonic frequencies from ref 45. [h] Fundamentals from ref 46.

$\alpha_{||}$, do not depend too sensitively on the method and the basis set applied. The only quantity that does depend strongly on the level of description is the polarizability perpendicular to the molecular axis (see last column of Table 1). With basis sets I and II and also with cc-pVDZ and cc-pVTZ the perpendicular polarizability is substantially underestimated. With the basis sets III, 6-311++G(3df,3dp), aug-cc-pVDZ, and aug-cc-pVTZ the computed values are to within a few percent of the experimental numbers, a consequence of the presence of the added diffuse functions, the *f*-functions being less important for that property. The proper description of the anisotropy of the molecular polarizability is a necessary ingredient when investigating the interaction energy at different dimer orientations. The computed values for $\alpha_{||}$ and $\alpha_{\perp}$ are in excellent agreement with the experimental values and agree also with earlier theoretical data.[49−51]

With the larger basis sets, the computed MP2 harmonic vibrational frequencies are reasonably close to the experimental harmonic frequencies, with the exception of the bending modes, which depend very strongly on the basis set saturation with higher angular momentum basis functions.[52] For all properties considered, the MP2/III and MP2(full)/III results are nearly identical.

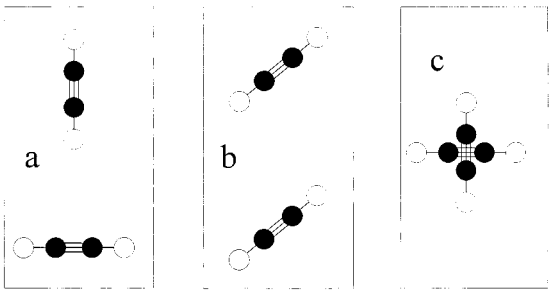

Figure 2. Stationary points of the acetylene dimer: π-type hydrogen-bonded C_{2v} minimum (a); slipped parallel C_{2h} first-order saddle point (b); D_{2d} second-order saddle point (c)

Diacetylene. The calculated data for the diacetylene monomer is shown in Table 3. Since the trends are very similar to the acetylene case, only the MP2 results as obtained with basis sets I−III, cc-pVTZ, and aug-cc-pVTZ are reported and confronted with experimental data or previous theoretical results. Again, as with the acetylene monomer, the computed structural properties, the quadrupole moment, and the parallel polarizability component, $\alpha_{||}$, are quite insensitive to basis set improvements. The perpendicular component of the polarizability, $\alpha_{\perp}$, is only well described with basis sets augmented with diffuse functions. Comparison between the MP2/III and MP2/aug-cc-pVTZ results shows again that f functions do not play too significant a role for the polarizabilities. The results as obtained with basis sets II and cc-pVTZ are, in general, very close.

The computed harmonic frequencies for the stretching modes are in quite good agreement with experimentally derived harmonic frequencies.[56] Again, agreement is less good for the bending modes and there the basis set dependence is substantial.

B. The Acetylene Dimer. In the case of the acetylene dimer, three stationary points bound relative to two isolated acetylene molecules were found on the energy surface. The structures are sketched in Figure 2. The C_{2v} structure with a π-type hydrogen bond (Figure 2a) is the minimum energy configuration ($\alpha = 0°$, $\beta = 90°$, $\gamma = 0°$), and the C_{2h} parallel slipped arrangement with $\alpha = \beta \approx 42°$ and $\gamma = 0°$ (Figure 2b) is a first-order saddle point, in agreement with practically all previous computations[7−10] and with experiment.[3,4,10] In addition to these two planar stationary points, a nonplanar structure with D_{2d} symmetry

TABLE 3: Computed Total Energies (*E*), Optimized Bond Distances, Rotational Constants (B_e), Quadrupole Moments (Θ), Parallel ($\alpha_{||}$) and Perpendicular ($\alpha_{\perp}$) Polarizabilities and Harmonic Vibrational Frequencies of the Diacetylene Monomer as Obtained at the MP2 Level Applying Different Basis Sets[a]

basis set	I	II	III	VI[b]	VIII[c]	experiment[d]
E [hartree]	−0.06929[a]	−0.11825	−0.12018	−0.15219	−0.16147	
r(H−C) [Å]	1.0622	1.0644	1.0643	1.0616	1.0623	1.062[e]
r(C≡C) [Å]	1.2143	1.2186	1.2190	1.2194	1.2202	1.206[e]
r(C−C) [Å]	1.3677	1.3704	1.3700	1.3686	1.3692	1.380[e]
B_e [GHz]	4.381	4.357	4.356	4.359	4.354	4.391[f]
Θ [debye Å]	11.90	12.64	12.57	12.55	12.63	12.16[g]
$\alpha_{||}$ [Å^3]	11.70	12.23	12.36	11.87	12.40	12.45[h]
$\alpha_{\perp}$ [Å^3]	2.77	3.67	4.46	3.34	4.48	4.47[h]
ω_1 (σ_g+)	3507	3465	3465	3491	3478	3489[i] (3332[j])
ω_2 (σ_g^+)	2210	2182	2179	2196	2185	2222 (2189)
ω_3 (σ_g^-)	900	892	892	898	897	885 (872)
ω_4 (σ_u^-)	3507	3465	3465	3490	3478	3490 (3333)
ω_5 (σ_u^-)	2027	2005	2001	2009	2001	2050 (2019)
ω_6 (π_g)	587	585	550	621	614	638 (626)
ω_7 (π_g)	214	389	316	481	460	490 (483)
ω_8 (π_u)	579	580	549	624	618	641 (628)
ω_9 (π_u)	182	204	195	229	218	223 (220)

[a] A value of −153.0 hartree to be added to each entry. [b] cc-pVTZ. [c] aug-cc-pVTZ. [d] Experimental data or previous theoretical data. [e] Estimated in ref 53. [f] Data from ref 54. [g] Data from ref 55. [h] MBPT2 results of ref 51. [i] Harmonic frequencies as reported in ref 56. [j] Fundamentals from refs 57 and 58.

TABLE 4: Optimized Structural Parameters of the Acetylene Dimer at the C_{2v}, C_{2h}, and D_{2d} Stationary Points

basis set	method	C_{2v} R [Å]	C_{2h} R [Å], α [deg]	D_{2d} R [Å]
I	MP2	4.34	4.32, 43.8	3.79
II	MP2	4.39	4.25, 42.8	4.01
III	MP2	4.32	4.22, 42.7	3.90
III	MP2(full)	4.31	4.21, 42.7	3.90
III	RHF	4.72	4.65, 43.4	unbound
III	B3LYP	4.51	4.52, 41.8	unbound
IV[a]	MP2	4.31	4.17, 43.3	3.83
V[b]	MP2	4.32	4.28, 42.2	4.16
VI[c]	MP2	4.33	4.23, 42.4	3.97
VII[d]	MP2	4.30	4.18, 42.2	3.87
VIII[e]	MP2	4.28	4.17, 42.5	3.87
experiment		4.38[f]		

[a] 6-311++G(3df,3pd). [b] cc-pVDZ. [c] cc-pVTZ. [d] aug-cc-pVDZ. [e] aug-cc-pVTZ. [f] Reference 3.

(Figure 2c) and $\alpha = \beta = \gamma = 90°$ turned out to be a second-order saddle point. The intramolecular structural relaxations taking place upon complex formation are weak in the acetylene dimer. At the stationary points, the computed bond length changes do not exceed 0.002 Å, and optimized bond angles deviate less than 0.5° from linearity. Hence, only the optimized intermolecular distance R, defined as the distance between the midpoints of the C≡C triple bonds (almost, but not quite identical to the center of mass separation), and the angle α (see Figure 1) for the C_{2h} structure are reported in Table 4.

The MP2 computed intermolecular distances R as obtained with the larger basis sets are about 4.3 Å for the C_{2v} minimum, 4.2 Å for the C_{2h} saddle point, and, with 3.9 Å, distinctly shorter for the D_{2d} second order saddle. The experimentally derived center of mass distance for the C_{2v} minimum is 4.4 Å.[4] The difference of about 0.1 Å between experimental and computed distances is most probably due to anharmonicity effects. The angle α in the C_{2h} structure is within a margin of 2° identical in all calculations, including RHF and B3LYP, indicating that the relative orientation is essentially already correctly described by the electrostatic interactions. In agreement with previous theoretical studies[6−10] and with the experimental analysis,[10] the optimal R values do not differ much in the C_{2v} and C_{2h} orientations. The center of mass separation is distinctly smaller in the D_{2d} arrangement. With DFT (B3LYP) and RHF the computed center of mass separations are consistently too large, a consequence of the lack of dispersion energy contributions. The D_{2d} structure is even unbound with B3LYP and RHF, i.e., optimization leads to infinitely separated molecules, a consequence of the repulsive electrostatic interaction energy in this relative orientation which is not properly counterbalanced in methods that cannot describe the dispersion energy.

The computed interaction energies, ΔE, the ZPE-corrected interaction energies, ΔE(ZPE), the BSSE-corrected interaction energies, ΔE(BSSE), and those corrected for both effects, ΔE(ZPE+BSSE), are reported in Tables 5−7 for the C_{2v}, C_{2h}, and D_{2d} structures, respectively. At the C_{2v} minimum, the raw interaction energies as obtained with the larger basis sets III, 6-311++G(3df,3dp), and aug-cc-pVTZ amount to −628, −653, and −691 cm^{-1}. Correcting only for ZPE effects results in values of −474, −492 and −514 cm^{-1}. Correcting for both ZPE and BSSE effects reduces these values to −353, −342, and −366 cm^{-1}, respectively. With all other basis sets the corrected interaction energies are too small in absolute value. This is particularly valid for the RHF and B3LYP results, which lead to nearly identical interaction energies amounting to only about one-third of the MP2 result obtained using the same basis set (III). As is well-known, the size of the BSSE correction is not directly related to the size of the basis set used. In our case, the BSSE correction happens to be smaller with basis set II than with basis set III. The same trend is observed when comparing cc- and aug-cc- basis sets. In agreement with many previous studies on intermolecular interactions, the BSSE correction is negligible at RHF and B3LYP levels when basis sets with diffuse functions are used. The MP2 and MP2(full) results as obtained with basis set III are practically identical. As a consequence of this feature, MP2(full) calculations have been dispensed with for the diacetylene dimer.

Essentially, all of the above trends are re-encountered in the C_{2h} and D_{2d} stationary points. Applying all corrections in the

TABLE 5: Computed Stabilization Energies (ΔE), ZPE-Corrected Stabilization Energies (ΔE(ZPE)), and BSSE-Corrected Stabilization Energies (ΔE(BSSE)) of the Acetylene Dimer at the C_{2v} Minimum[a]

basis set	method	ΔE	ΔE(ZPE)	ΔE(BSSE)	ΔE(ZPE+BSSE)
I	MP2	−541	−365	−288	−112
II	MP2	−519	−377	−459	−317
III	MP2	−628	−474	−507	−353
III	MP2(full)	−653	−498	−507	−352
III	RHF	−252	−134	−249	−131
III	B3LYP	−267	−132	−264	−129
IV[b]	MP2	−652	−492	−503	−342
V[c]	MP2	−617	−430	−405	−218
VI[d]	MP2	−571	−429	−480	−339
VII[e]	MP2	−856	−613	−483	−239
VIII[f]	MP2	−691	−514	−543	−366

[a] All values in cm^{-1}. [b] 6-311++G(3df,3pd). [c] cc-pVDZ. [d] cc-pVTZ. [e] aug-cc-pVDZ. [f] aug-cc-pVTZ.

TABLE 6: Computed Stabilization Energies (ΔE), ZPE-Corrected Stabilization Energies (ΔE(ZPE)), and BSSE-Corrected Stabilization Energies (ΔE(BSSE)) of the Acetylene Dimer at the C_{2h} Saddle Point[a]

basis set	method	ΔE	ΔE(ZPE)	ΔE(BSSE)	ΔE(ZPE+BSSE)
I	MP2	−396	−319	−257	−181
II	MP2	−464	−352	−415	−303
III	MP2	−535	−428	−457	−350
III	MP2(full)	−550	−446	−457	−353
III	RHF	−201	−112	−201	−112
III	B3LYP	−176	−87	−168	−79
IV[b]	MP2	−573	−457	−475	−358
V[c]	MP2	−518	−398	−322	−202
VI[d]	MP2	−510	−394	−433	−317
VII[e]	MP2	−693	−531	−452	−290
VIII[f]	MP2	−588	−476	−509	−397

[a] All values in cm^{-1}. [b] 6-311++G(3df,3pd). [c] cc-pVDZ. [d] cc-pVTZ. [e] aug-cc-pVDZ. [f] aug-cc-pVTZ.

TABLE 7: Computed MP2 Stabilization Energies (ΔE), ZPE-Corrected Stabilization Energies (ΔE(ZPE)), and BSSE-Corrected Stabilization Energies (ΔE(BSSE)) of the Acetylene Dimer at the D_{2d} Second-Order Saddle Point[a]

basis set	ΔE	ΔE(ZPE)	ΔE(BSSE)	ΔE(ZPE+BSSE)
I	−118	−90	21	48
II	−93	−76	−44	−27
III	−149	−126	−74	−51
III[b]	−162	−137	−74	−49
IV[c]	−153	−135	−81	−63
V[d]	−46	−28	56	75
VI[e]	−90	−69	−25	−5
VII[f]	−157	−143	−61	−46
VIII[g]	−155	−131	−105	−81

[a] All values in cm^{-1}. [b] MP2 (full). [c] 6-311++G(3df,3pd). [d] cc-pVDZ. [e] cc-pVTZ. [f] aug-cc-pVDZ. [g] aug-cc-pVTZ.

TABLE 8: Computed Energy Differences $\Delta\Delta E$ between C_{2h} Saddle Point and C_{2v} Minimum of the Acetylene Dimer[a]

basis set	method	$\Delta\Delta E$	$\Delta\Delta E$(ZPE)	$\Delta\Delta E$(BSSE)	$\Delta\Delta E$(ZPE+BSSE)
I	MP2	145	66[b] (46)[c]	31	−49 (−69)[b]
II	MP2	55	49 (25)	44	28 (14)
III	MP2	93	62 (46)	50	19 (3)
III	MP2(full)	103	69 (52)	50	16 (−1)
III	RHF	50	33 (21)	47	30 (18)
III	B3LYP	92	61 (45)	96	66 (50)
IV[d]	MP2	80	51 (35)	28	0 (−16)
V[e]	MP2	99	50 (32)	83	34 (16)
VI[f]	MP2	60	49 (35)	48	36 (22)
VII[g]	MP2	163	101 (82)	31	−32 (−51)
VIII[h]	MP2	103	54 (37)	34	−15 (−32)

[a] All values in cm^{-1}. [b] Values obtained with ZPE correction but without that of the lowest b_2 mode of the C_{2v} minimum. [c] Values in parentheses as obtained including the lowest b_2 mode of the C_{2v} minimum. [d] 6-311++G(3df,3pd). [e] cc-pVDZ. [f] cc-pVTZ. [g] aug-cc-pVDZ. [h] aug-cc-pVTZ.

TABLE 9: Computed Stabilization Energies of the Acetylene Dimer with Different Electron Correlation Methods[a,b]

	basis sets								
	III			IV[c]			VIII[d]		
method	C_{2v}	C_{2h}	D_{2d}	C_{2v}	C_{2h}	D_{2d}	C_{2v}	C_{2h}	D_{2d}
MP2	−628	−535	−149	−652	−573	−153	−691	−588	−155
MP3	−561	−451	−66	−586	−489	−61	−611	−490	−62
MP4(D)	−564	−461	−82	−591	−501	−79	−617	−503	−80
MP4(DQ)	−511	−421	−39	−533	−453	−27	−556	−454	−32
MP4(SDQ)	−492	−407	−18	−512	−435	−2	−536	−437	−8
MP4(SDTQ)	−585	−489	−95	−612	−528	−88	−644	−540	−94
CCD	−504	−413	−43	−529	−449	−35	−551	−448	−38
CCSD	−491	−405	−24	−514	−436	−5	−537	−437	−16
CCSD(T)	−572	−473	−84	−599	−511	−76	−629	−519	−81

[a] All values in cm^{-1}. [b] All calculations performed at MP2 optimized structures with the given basis set. [c] 6-311++G(3df,3pd). [d] aug-cc-pVTZ.

case of the D_{2d} structure leads even to positive (repulsive) interaction energies with the smaller basis sets.

Of particular interest is the energy difference between the C_{2h} saddle and the C_{2v} minimum ($\Delta\Delta E$). This is the barrier height in the potential for the *geared* rotation. The experimental estimate for $\Delta\Delta E$ amounts to 33 cm^{-1}, about 0.1 kcal mol^{-1}.[10] In previous theoretical results,[9,13] as obtained within the framework of the MP2 approximation, values of 20 and 47 cm^{-1} were reported for this quantity. In the work of Bone and Handy[20] a basis set comparable to basis set II was used, and BSSE and ZPE corrections were evaluated. In the calculations of Resende and DeAlmeida,[13] a basis set close to basis set I was applied. BSSE corrections were evaluated, but ZPE corrections were not. The $\Delta\Delta E$ energy differences calculated in this work are shown in Table 8. Inspecting the uncorrected and ZPE corrected interaction energy differences, one observes a quite uniform trend. The larger basis set MP2 results (III, IV, VIII) lead to uncorrected energy differences in the range from 80 to 103 cm^{-1}. The corresponding ZPE-corrected values range from 51 to 62 cm^{-1}, a slightly narrower regime. However, inclusion of the full BSSE correction strongly perturbs the picture, leading to values from 19 to −32 cm^{-1} and thus to a reversal of the relative stabilities with the aug-cc-pVTZ basis. It is probably fair to say that the MP2 approximation in combination with basis sets augmented with diffuse functions, with the harmonic approximation for ZPE corrections, and with the still sizable and still somewhat irregularly behaving BSSE correction is not capable to describe the interaction energy with a precision of a few cm^{-1}.

The effect of going beyond the MP2 approximation is illustrated in Table 9. There, the interaction energies as obtained with MP3, with different MP4 variants, and with CCD, CCSD, and CCSD(T) are compiled. These calculations were performed at the MP2 optimized structures for the acetylene monomer and at the stationary points of the acetylene dimer for each basis set. Only the results as obtained with the three largest basis sets are reported.

In agreement with previous studies on the acetylene dimer[11] and also with calculations on the benzene dimer,[59−61] MP2 slightly overestimates the stabilization energies in absolute value. However, comparing the MP2 stabilization energies with those obtained using MP4(SDTQ) and CCSD(T) approaches shows that the differences are modest only and nearly constant (50−70 cm^{-1} between MP2 and CCSD(T) and about 10−20 cm^{-1} between MP4(SDTQ) and CCSD(T)) for all three configurations and for all three basis sets, at least when freezing the MP2 equilibrium structures. As a consequence of this behavior, the very costly electron correlation calculations beyond MP2 were dispensed with for the case of the diacetylene dimer.

The MP2 computed harmonic frequencies for the three stationary points as obtained with the three largest basis sets are compiled in Table 10. The intermolecular vibrational frequencies and the frequency shifts of the intramolecular vibrations relative to the corresponding monomer vibrations are reported. Despite the large variations in the calculated harmonic frequencies for the bending modes, the frequency shifts are expected to be significantly less sensitive to the basis set applied. The experimental acetylene monomer fundamentals are included in Table 10. With all three basis sets, the predicted shifts are quite similar. In the case of the C_{2v} minimum and the C_{2h} saddle, the calculated shifts agree well with earlier theoretical results.[7,9] Experimental shifts for some of the intramolecular vibrations of the acetylene dimer amount to +8 and −2 cm^{-1} for ω_4 and ω_2,[1] +7 cm^{-1} for ω_5,[5] and −16 cm^{-1} for ω_3, respectively.[2−4]

Summarizing the acetylene dimer results obtained in this work, we observe quite reasonable agreement with the experimental data. The MP2/III frozen core level of approximation results in satisfactory structures, stabilization energies, frequency shifts, and in an overall acceptable description of the intermolecular energy surface. The accurate prediction of the C_{2v} −

TABLE 10: Computed Harmonic Intermolecular Vibrational Frequencies of the Acetylene Dimer and Frequency Shifts of the Intramolecular Dimer Vibrations Relative to the Acetylene Monomer[a]

	C_{2v}				C_{2h}				D_{2d}			
basis set		III	IV[b]	VIII[c]		III	IV	VIII		III	IV	VIII
intermolecular	b_2	31	32	34	b_u	24i	18i	17i	e	45i	48i	45i
	b_1	54	67	77	a_u	41	42	46	b_1	41	42	43
	a_1	80	82	86	a_g	50	53	53	a_1	39	43	40
	b_2	102	100	106	a_g	119	126	128				
intramolecular relative to[d]												
ω_4 (612)[e]	a_2	3	−1	2	b_g	3	3	5	e	−11	−15	−9
	b_2	4	5	5	b_u	0	2	−1	a_2	−1	−5	1
	b_1	5	11	18	a_u	5	5	5	b_1	2	−2	3
	b_2	26	21	23	a_g	9	9	5	b_2	−13	−10	−8
ω_5 (730)	b_1	−3	−1	0	b_u	−2	1	0	a_1	−6	−5	−3
	a_1	5	7	8	b_g	−1	0	2	e	−1	1	1
	b_1	16	23	30	a_g	6	9	10	b_2	−1	−1	−2
	b_2	32	29	35	a_u	7	8	10	a_1	−1	−2	−2
ω_2 (1974)	a_1	−6	−7	−7	a_g	−4	−5	−5	e	2	0	−2
	a_1	−2	−3	−3	b_u	−2	−3	−3	b_2	1	0	−4
ω_3 (3289)	a_1	−20	−22	−23	a_g	−4	−7	−9	a_1	1	0	−3
	b_2	−4	−6	−8	b_u	−4	−7	−9				
ω_1 (3374)	a_1	−13	−15	−19	a_g	−4	−6	−9				
	a_1	−4	−6	−12	b_u	−4	−6	−9				

[a] All values in cm^{-1}. [b] 6-311++G(3df,3dp). [c] aug-cc-pVTZ. [d] Shifts relative to the corresponding acetylene monomer frequencies (see Table 2). [e] Experimental frequencies of the acetylene monomer.

C_{2h} energy difference to a few cm^{-1} is, however, still unachievable with the current approach.

C. The Diacetylene Dimer. From extended scans of the energy surface of the diacetylene dimer at MP2/I and MP2/II levels, six high-symmetry stationary points emerged. Five out of these six have planar structures; one is a nonplanar arrangement. These are definitely not all stationary points. A complete search for all conceivable bound stationary states including their characterization is, however, beyond the scope of this work. The high-symmetry stationary points of the diacetylene dimer detected and investigated in this work are shown in Figure 3. These were subjected to complete geometry optimizations with basis sets I−III. Vibrational analyses were performed with basis sets I and II. MP2/III vibrational analysis surpassed the available computing resources by far.

Structure 3a has C_{2v} symmetry and a hydrogen bond directed toward the central single bond of the partner diacetylene molecule. It is a first-order saddle point. Structure 3b has C_s symmetry and a tilted, π-type hydrogen-bonded structure. It is a minimum on the energy surface. Structures 3c and 3e are slipped parallel, stacked structures and have C_{2h} symmetry. Both are minima on the energy surface. Interestingly, 3e is the only minimum detected in a recent DFT investigation on the dimer of diacetylene.[15] Structure 3d has D_{2h} symmetry and is a second-order saddle point. Its counterpart in the acetylene dimer case is unbound at all levels of approximation. Configuration 3f has D_{2d} symmetry and it is a minimum, whereas its counterpart in the acetylene dimer is a second-order saddle point, as discussed in a previous section.

Although the intramolecular structure relaxations taking place upon complex formation are a bit larger than in the case of the acetylene dimer, they are still small in the diacetylene dimer. With the largest basis set, III, bond angle distortions amount mostly only to a few tenths of a degree, and are always below 2° for all stationary points considered. Bond length distortions again do not exceed 0.002 Å. In Table 11, the optimized intermolecular geometry, ($R/\alpha/\beta/\gamma$), is shown as obtained with basis sets I, II, and III at the MP2 level for the six stationary points. R is defined as the distance between the midpoints of the central C−C single bonds. The computed stabilization energies of the diacetylene dimer are compiled in Table 12.

Before discussing the structures and energetics of the stationary points in detail, a few general trends can be observed. The optimized structural parameters are not very sensitive to the basis set applied. For a given structure type, the computed R values differ by less than 0.1 Å. The calculated α and β values are also very close, even if not predetermined by symmetry. The BSSE corrections are largest with basis set I, smallest with basis set II, and larger again with basis set III. The same pattern was observed in the acetylene dimer case. Application of the BSSE correction does not appear to be advisable when using basis set I. Evidently, one rather destroys an error compensation (large BSSE correction versus underestimation of dispersion energy) than to improve the results.

Structures 3a and 3b are related to the C_{2v} minimum of the acetylene dimer, where one monomer acts as a hydrogen bond donor and the other as a hydrogen bond acceptor. Formally, 3a is a saddle point between two energetically degenerate structures 3b. The computed energy difference, in particular when corrected for ZPE and BSSE effects, between these two structures is, however, exceedingly small, too small for a definitive assessment as to which is the more stable. In any case, one has to expect a large amplitude motion in the coordinate which transforms structure 3b to structure 3a and again to an energetically equivalent structure 3b. Indeed, the computed lowest harmonic vibrational frequency of the C_s structure 3b is computed as 14 and 9 cm^{-1} with basis sets I and II, respectively. It has an eigenvector fitting to that of the imaginary frequency of 3a (35i and 29i with basis sets I and II). At the present stage, it is still unclear whether 3b can actually sustain a bound state relative to 3a in this shallow double minimum potential.

Structure 3c appears to be the global minimum on the intermolecular energy surface of the diacetylene dimer. It is about −70 cm^{-1} more stable than 3a,b and 3f and about −120 cm^{-1} more stable than 3e, when considering MP2/III ΔE(ZPE+BSSE) values. The corresponding MP2/II results are very similar, whereas the MP2/I ΔE(ZPE+BSSE) show a different energetic ordering of the stationary points, a consequence of the very large BSSE correction. The C_{2h}-symmetric minima 3c and 3f are reminiscent of the C_{2h} saddle point of the acetylene dimer. There, the setting angle $\alpha = \beta$ is about 43°. In 3c, $\alpha = \beta$ is about 62°, in 3e it amounts to about 31°. The center of

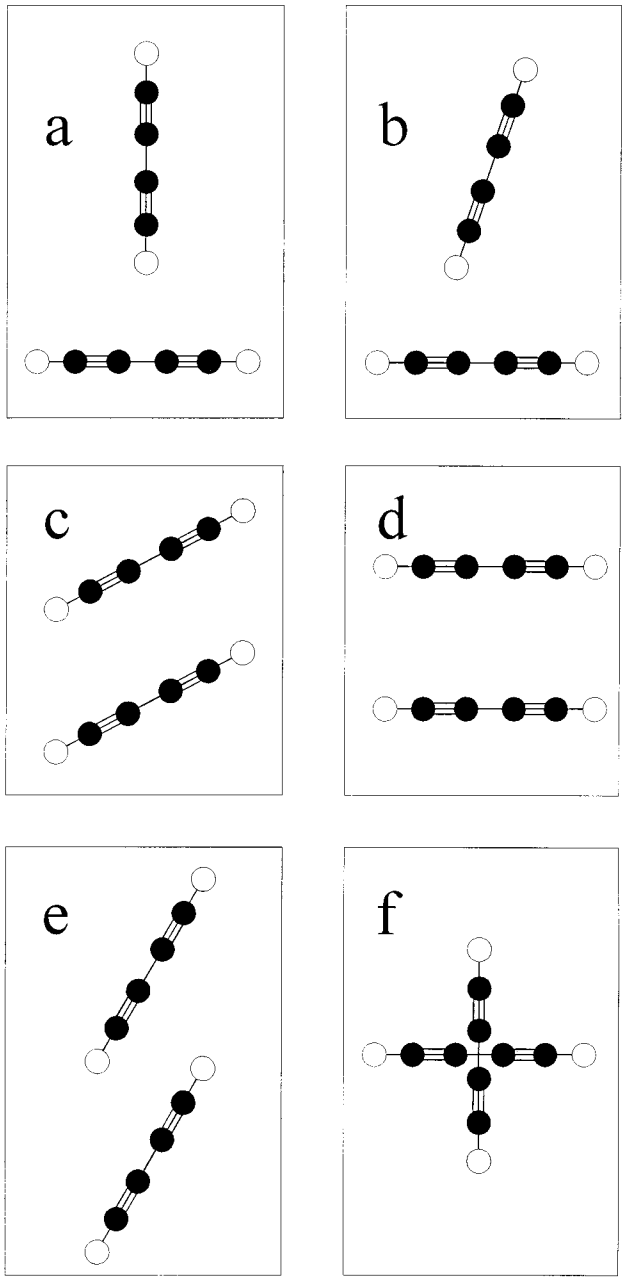

Figure 3. Stationary points of the diacetylene dimer: C_{2v} hydrogen-bonded structure (a); C_s tilted, π-type hydrogen-bonded structure (b); C_{2h} slipped parallel, stacked structure with $\alpha = \beta \approx 60°$ (c); D_{2h} parallel stacked structure (d); C_{2h} slipped parallel, stacked structure with $\alpha = \beta \approx 30°$ (e); D_{2d} configuration (f).

TABLE 11: MP2-Optimized Structural Parameters ($R/\alpha/\beta/\gamma$) of the Diacetylene Dimer at Different Stationary Points[a]

	basis sets		
structure	I	II	III
3a, C_{2v}	5.56/90/0/0	5.63/90/0/0	5.58/90/0/0
3b, C_s	5.36/93.1/−16.7/0	5.43/93.0/−16.8/0	5.37/93.5/−16.8/0
3c, C_{2h}	3.92/62.6/62.6/0	3.90/62.0/62.0/0	3.88/62.0/62.0/0
3d, D_{2h}	3.80/90/90/0	3.84/90/90/0	3.78/90/90/0
3e, C_{2h}	5.99/32.4/32.4/0	6.02/30.7/30.7/0	5.99/30.5/30.5/0
3f, D_{2d}	3.23/90/90/90	3.33/90/90/90/	3.29/90/90/90

[a] R in angstroms; α, β, and γ in degrees.

mass separation is radically different in these two structures, with about 3.9 Å in 3c and about 6 Å in 3e, whereas it is about 4.2 Å in the C_{2h} saddle point of the acetylene dimer.

TABLE 12: Computed MP2 Stabilization Energies (ΔE), ZPE-Corrected Stabilization Energies (ΔE(ZPE)), ZPE-Correction (ZPE), BSSE-Corrected Stabilization Energies (ΔE(BSSE)), and BSSE-Correction (BSSE) of the Diacetylene Dimer at Different Stationary Points[a]

structure	basis set	ΔE	ΔE(ZPE)	ZPE	ΔE(BSSE)	BSSE	ΔE(ZPE+BSSE)
3a, C_{2v}	I	−646	−609	38	−244	403	−206
	II	−621	−582	39	−535	86	−496
	III[b]	−782	−743		−601	180	−563
3b, C_s	I	−701	−564	137	−299	403	−162
	II	−656	−580	57	−566	90	−490
	III[b]	−831	−756		−635	196	−560
3c, C_{2h}	I	−701	−719	−18	−145	556	−162
	II	−712	−680	32	−576	136	−544
	III[b]	−875	−844		−662	214	−630
3d, D_{2h}	I	−344	−437	−93	212	556	119
	II	−325	−340	−16	−230	94	−246
	III[b]	−456	−472		−299	158	−314
3e, C_{2h}	I	−523	−465	58	−292	231	−234
	II	−581	−581	64	−518	63	−453
	III[b]	−682	−618		−574	108	−510
3f, D_{2d}	I	−924	−870	54	71	995	125
	II	−661	−642	20	−494	168	−474
	III[b]	−880	−860		−584	295	−565

[a] All values in cm^{-1}. [b] ZPE corrections taken over from MP2/II calculations.

Taking into account that its counterpart in the acetylene dimer is a second-order saddle point only, the D_{2d} structure 3f with an orthogonal orientation of the two molecules is surprisingly stable, about as stable as the hydrogen-bonded structures 3a,b. Among the minima, it has with about 3.3 Å the smallest center of mass separation by far. Despite the electrostatically unfavorable monomer orientation, structure 3d is still bound by almost 1 kcal mol^{-1}.

Since experimental vibrational spectroscopic data are not yet available for the diacetylene dimer, the computed vibrational spectra stand as predictions. The intermolecular vibrational frequencies and the shifts of the intramolecular frequencies relative to the corresponding monomer vibrations for the four minima [3b (C_s), 3c (C_{2h}), 3e (C_{2h}), 3f (D_{2d})] are collected in Table 13. Only the data as obtained at the MP2/II level are reported. Among the C−H stretching frequencies, only one large frequency shift of -24 cm^{-1} is obtained for the hydrogen-bonded C−H group in the C_s conformation (structure 3b). The corresponding shift for the C_{2v} saddle point (structure 3a) with the hydrogen bond oriented toward the C−C single bond of the partner molecule amounts to -11 cm^{-1} only. The only larger shifts in the C_s conformation stem from CCH bending modes. In general, all shifts originating from C−H, C≡C, and C−C stretching modes are significantly below 10 cm^{-1}, with the exception of the above-mentioned hydrogen-bonded C−H group vibration. The shifts in the intramolecular bending modes are slightly larger, but, with the exception of the C_s structure, do not exceed 20 cm^{-1} in absolute value. Probably, it will be quite difficult to discern between the various structural alternatives from the experimental side on the basis of the gas-phase vibrational frequencies alone. Therefore, the theoretical rotational constants (MP2/II) are reported in Table 14. The values for the rotational constants indeed appear to be sufficiently different to allow discrimination of the different structures.

D. Comparison of the Energy Surfaces of the Two Dimers. To give an impression of some relevant sections of the energy surfaces, contour plots of selected 2D cuts are shown. Throughout, these were obtained from MP2/II energies uncorrected for BSSE. The scans were performed with a 10° mesh in the angular coordinates and with 0.25 Å increments in R.

TABLE 13: Computed Harmonic Intermolecular Vibrational Frequencies at the Four Minima of the Diacetylene Dimer and Frequency Shifts of the Intramolecular Dimer Vibrations Relative to the Diacetylene Monomer as Obtained at the MP2/II Level[a]

structure	3b, C_s	3c, C_{2h}	3e, C_{2h}	3f, D_{2d}
intermolecular	9	11	13	15
	21	39	16	36
	39	49	20	59
	63	80	81	
intramolecular relative to[b]				
ω_9 (220)[c]	−2, −1, 1, 9	−3, −1, 0, 1	1, 2, 3, 9	−7, −3, −2
ω_7 (490)	−4, −1, −1, −1	−9, −9, −7, −5	−3, −3, −2, −2	−8, −8, −5
ω_6 (626)	−5, −4, −2, 9	−17, −12, −12, −9	−3, −1, 0, 1	−10, −8, −5
ω_8 (628)	0, 4, 23, 32	−9, −1, −3, −5	−2, 3, 5, 12	−7, −3, −3
ω_3 (872)	1, 1	1, 1	1, 1	1, 1
ω_5 (2019)	−3, −2	−4, −4	−2, −2	−3
ω_2 (2189)	−4, −1	−6, −3	−3, −1	−3, −2
ω_1 (3332)	−24, −4	−1, 0	−5, −5	1
ω_4 (3333)	−2, 2	2, 2	0,0	1, 1

[a] All values in cm^{-1}. [b] Shifts relative to the corresponding diacetylene monomer frequencies (see Table 3). [c] Experimental frequencies of the diacetylene monomer.

TABLE 14: Theoretical Rotational Constants for the Four Minima of the Diacetylene Dimer[a]

structure	3b, C_s	3c, C_{2h}	3e, C_{2h}	3f, D_{2d}
A	4.098	3.444	10.13	2.179
B	0.599	1.089	0.464	1.284
C	0.523	0.827	0.444	1.284

[a] All values in gigahertz.

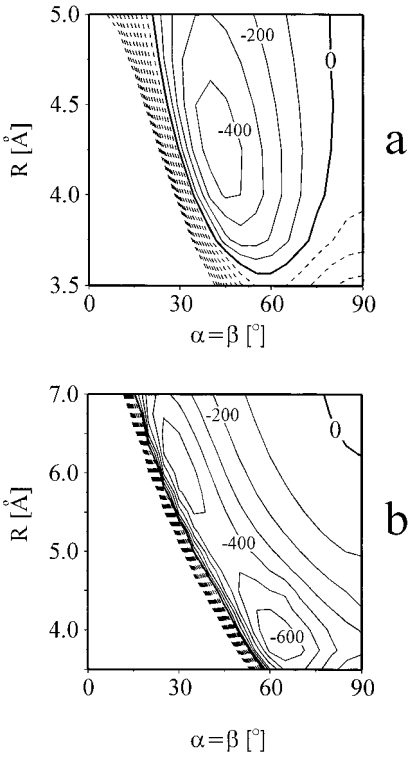

Figure 4. Contour plots for C_{2h} symmetry-retaining intermolecular motions ($\gamma = 0$) in the acetylene dimer (a) and in the diacetylene dimer (b). Successive contour lines in units of 100 cm^{-1}. The zero-energy contour is drawn with a thicker line. Full lines for attractive regions, broken lines for repulsive regions. Contours are drawn from −600 to +1000 cm^{-1}.

In the following, the 2D cuts through the 4D intermolecular energy surface of the diacetylene dimer are always compared to corresponding plots of the acetylene dimer in order to illustrate similarities and dissimilarites between the two dimers. As in the first example, cuts retaining C_{2h} symmetry throughout (R versus $\alpha = \beta$; $\gamma = 0$) for planar configurations are shown in Figure 4. The difference between the two cases is immediately visible. One minimum (actually the C_{2h} saddle) occurs in the case of the acetylene dimer (see Figure 4a), whereas two minima exist for the diacetylene dimer (minima 3c and 3e), with the less canted structure 3c more stable than 3e, and both being deeper than the basin in the acetylene dimer.

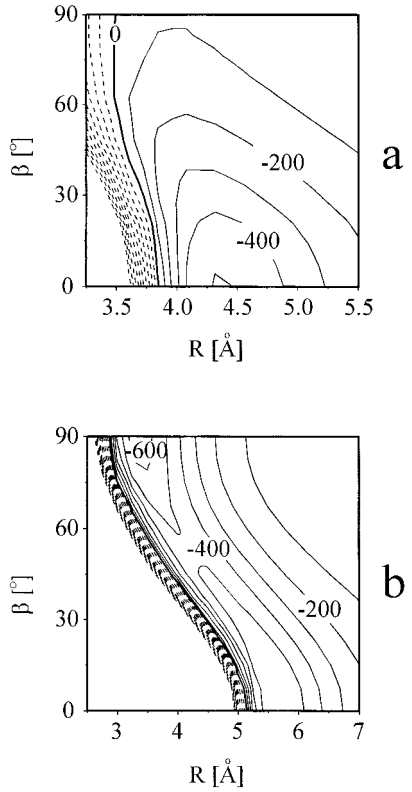

Figure 5. Contour plots for the transition from C_{2v} ($\alpha = 90°$, $\beta = 0°$, $\gamma = 90°$) to D_{2d} structures ($\alpha = 90°$, $\beta = 90°$, $\gamma = 90°$) in the acetylene dimer (a) and in the diacetylene dimer (b). Successive contour lines in units of 100 cm^{-1}. The zero-energy contour is drawn with a thicker line. Full lines for attractive regions, broken lines for repulsive regions. Contours are drawn from −600 to +1000 cm^{-1}.

Next, we consider the transition from the planar π-type hydrogen-bonded C_{2v} arrangements to the orthogonally oriented D_{2d} structures. This is shown in Figure 5. This pathway may be viewed as starting at $\beta = 0°$ (C_{2v}) and ending at at $\beta = 90°$ (D_{2d}) with α and γ simultaneously constrained to 90° throughout. In the acetylene dimer (Figure 5a), a minimum occurs for

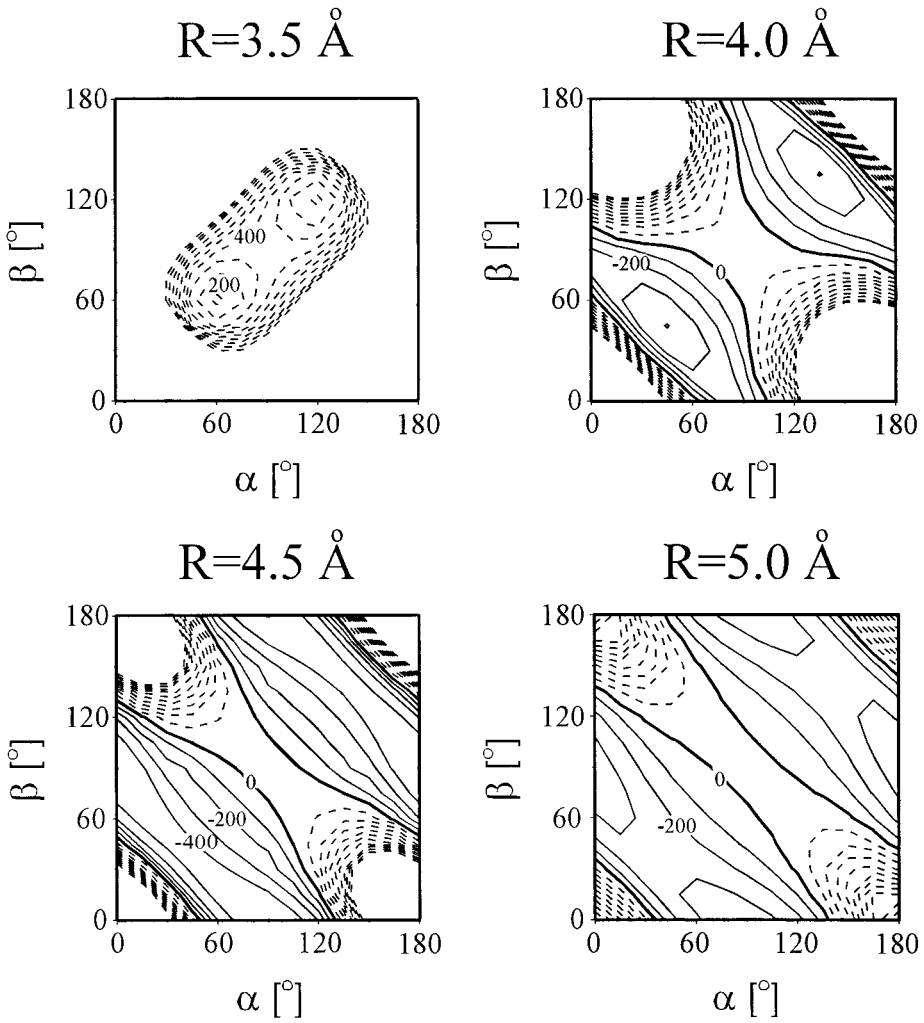

Figure 6. Contour plots for in-plane rotations ($\gamma = 0$) of the acetylene dimer for four different values of the center of mass distance *R*. Successive contour lines in units of 100 cm^{-1}. The zero-energy contour is drawn with a thicker line. Full lines for attractive regions, broken lines for repulsive regions. Contours are drawn from -400 to $+1000$ cm^{-1}.

$\beta = 0°$ and a saddle point for $\beta = 90°$. In the diacetylene dimer (Figure 5b), minima occur for $\beta = 0°$ and for $\beta = 90°$ with a comparatively low-lying saddle point at $\beta \approx 52°$ which has, however, not been investigated further in this work.

Finally, contour plots for in-plane rotations (α and β varying; $\gamma = 0$) for different values of *R* are shown in Figures 6 and 7. Because of symmetry, only a quarter of the plotted regions is nonreduntant. A number of general features can be observed when comparing the two cases. For shorter distances, $R = 3.5$ Å and $R = 4.0$ Å, the structures with $\alpha = \beta$ are preferred. This is a trivial steric effect. For these shorter distances, the interaction energy is much more attractive in the case of the diacetylene dimer than for the acetylene dimer. This is largely due to the more attractive dispersion energy contribution in the diacetylene dimer, to a lesser degree obviously also to the larger BSSE effect in the diacetylene dimer. In general, the structures with D_{2h} symmetry (α,β) = (90,90) are at repulsive energies in the acetylene dimer and at attractive energies in the diacetylene dimer. At about 4.25 Å, the energy surfaces of both dimers start to bifurcate, with lower energies for configurations with $\alpha \neq \beta$. This tendency is present in both cases. However, in the case of the acetylene dimer, the optimal distance occurs already somewhat below 4.5 Å. The *geared* rotation of the two acetylene molecules takes place in the narrow strips with $\alpha + \beta = 90°$ and 270°, respectively, the π-type hydrogen-bonded configuration with (α,β) = (0,90) or (90,0) being slightly lower in energy than the slipped parallel structure with (α,β) = (45,45). In the diacetylene dimer, on the other hand, the bifurcation tendency is more evident, with minima corresponding to tilted, π-type hydrogen-bonded configurations having their maximal depth at *R* values slightly below 5.5 Å. The minimum corresponding to the higher-lying C_{2h} structure is not clearly visible since with frozen monomers it develops at values larger than $R = 6.0$ Å. Thus, already the in-plane dynamics of the diacetylene dimer is much more complicated than that of the acetylene dimer. Instead of being confined to the comparatively narrow low-energy configuration space of the acetylene dimer with a nearly constant center of mass distance *R*, minima of comparable depth occur for very different values of *R* in the case of the diacetylene dimer.

Summary and Conclusions

A large-scale systematic study of the energy surfaces of two dimers, the dimer of acetylene molecules and the dimer of diacetylene molecules, has been performed in this work. In both cases, the most relevant stationary points have been fully geometry-optimized and characterized via vibrational analysis. The data presented for the acetylene dimer were obtained at a higher theoretical level than in previous theoretical investigations. The general picture of a dimer with an essentially in-plane dynamical behavior, consisting of a *geared* rotation of

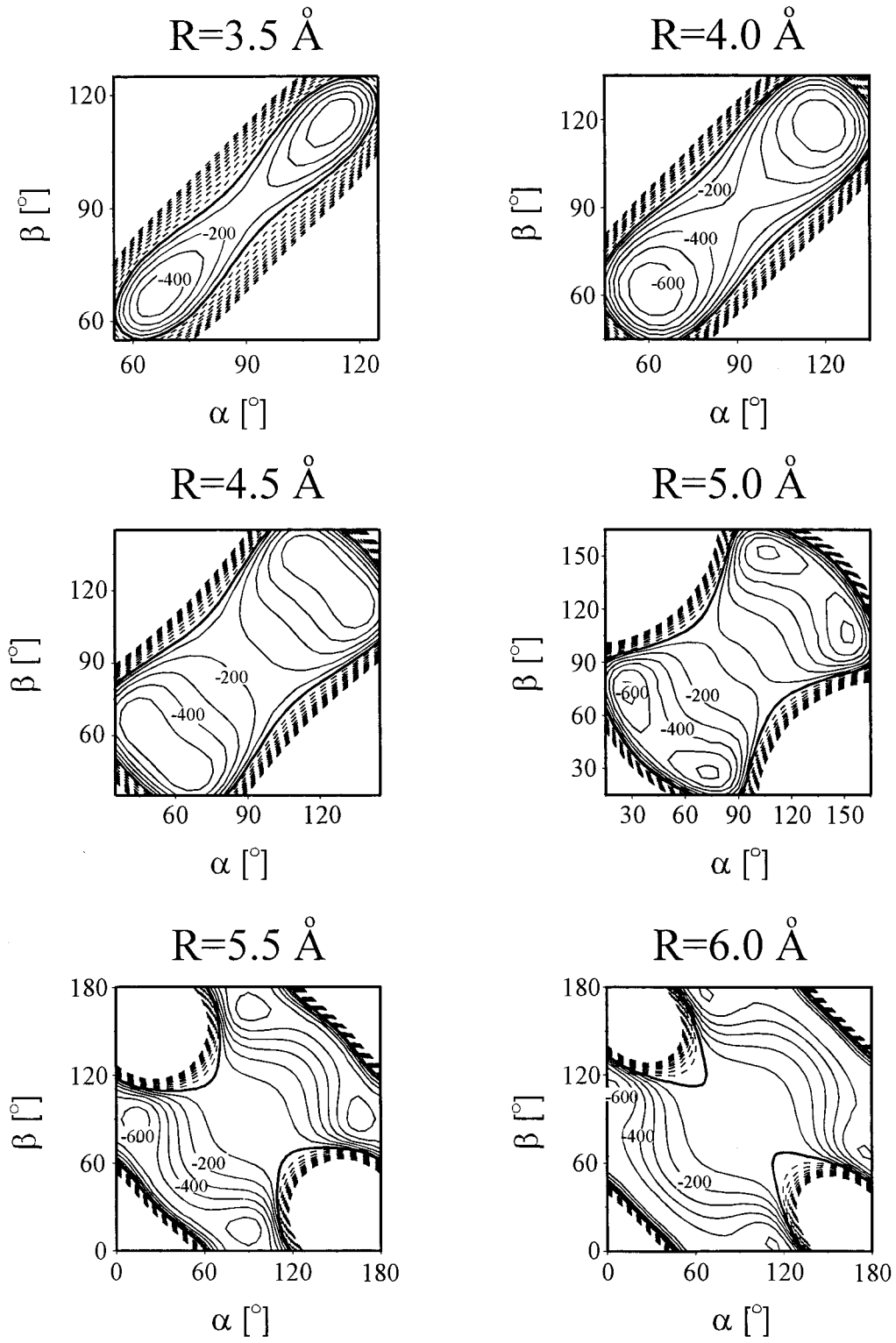

Figure 7. Contour plots for in-plane rotations ($\gamma = 0$) of the diacetylene dimer for six different values of the center of mass distance *R*. Successive contour lines in units of 100 cm^{-1}. The zero-energy contour is drawn with a thicker line. Full lines for attractive regions, broken lines for repulsive regions. Contours are drawn from -600 to $+1000$ cm^{-1}.

the two molecules with a nearly constant center of mass distance, and a small energy difference between the C_s minimum and the C_{2h} saddle point confirms earlier experimental and theoretical studies. Additionally, a further second-order saddle point with D_{2d} symmetry has been located.

The dimer of diacetylene displays a much richer-structured energy surface. The global minimum is a C_{2h}-symmetric slipped parallel structure with $\alpha = \beta \approx 62°$, a center of mass distance of about 3.9 Å and an interaction energy close to -630 cm^{-1} at the MP2/III level after correcting for BSSE and ZPE effects. Next in energy, about 70 cm^{-1} less favorable, is a planar, tilted, π-type hydrogen-bonded structure having C_s symmetry with the hydrogen bond donor molecule pointing at the center of one of the two C≡C triple bonds of the hydrogen bond acceptor molecule. The C_{2v} "σ-type" hydrogen-bonded structure with the hydrogen bond donor pointing at the center of the C−C single

bond of the acceptor is, however, only at slightly higher energies. This shallow double minimum potential certainly gives rise to large amplitude motions. Almost energetically degenerate with the C_s minima is a nonplanar D_{2d} configuration in which the two diacetylene molecules are orthogonally oriented. A fourth low-lying minimum, again of C_{2h} symmetry, with $\alpha = \beta \approx 30°$, about 120 cm^{-1} higher than the global minimum complicates the energy surface further.

So far, there are neither experimental data nor previous theoretical calculations available for this dimer. The theoretical structural and spectroscopic results presented in this work, hence, must stand as predictions. It appears that the dimer of diacetylene molecules is a very interesting model system because of the rich-structured energy surface and because of the energetically close-lying minima and the low-lying saddle points between them. As the first member of the series of molecules with conjugated triple bonds, this dimer is also an ideal testing ground for still advanced theoretical investigations. The detailed determination of the various minimum energy pathways for the interconversion of the different minima remains a challenging task for future investigations.

Acknowledgment. The calculations were performed on the Cluster of Digital Alpha Servers (2100 4/275 and 5/375) of the computer center of the University of Vienna and on local RISC 6000/550 and Silicon Graphics workstations at the Institute of Theoretical Chemistry and Radiation Chemistry of the University of Vienna. The author is grateful for an ample supply of computer time on these installations.

References and Notes

(1) Pendley, R. D.; Ewing, G. E. *J. Chem. Phys.* **1983**, *78*, 3531.
(2) Fischer, G.; Miller, R. E.; Vohralik, P. F.; Watts, R. O. *J. Chem. Phys.* **1985**, *83*, 1471.
(3) Prichard, D. G.; Nandi, R. N.; Muenter, J. S. *J. Chem. Phys.* **1988**, *89*, 115.
(4) Fraser, G. T.; Suenram, R. D.; Lovas, F. J.; Hougen, J. T.; Lafferty, W. J.; Muenter, J. S. *J. Chem. Phys.* **1988**, *89*, 6028.
(5) Ohshima, Y.; Matsumoto, Y.; Takami, M.; Kuchitsu, K. *Chem. Phys. Lett.* **1988**, *147*, 1.
(6) Aoyama, M.; Matsuoka, O.; Nakagawa, N. *Chem. Phys. Lett.* **1979**, *67*, 508.
(7) Alberts, I. L.; Rowlands, T. W.; Handy, N. C. *J. Chem. Phys.* **1988**, *88*, 3811.
(8) Craw, J. S.; De Almeida, W. B.; Hinchliffe, A. *J. Mol. Struct. (THEOCHEM)* **1989**, *201*, 69.
(9) Bone, R. G. A.; Handy, N. C. *Theor. Chim. Acta* **1990**, *78*, 133.
(10) Muenter, J. S. *J. Chem. Phys.* **1991**, *94*, 2781.
(11) Hobza, P.; Selzle, H. L.; Schlag, E. W. *Collect. Czech. Chem. Commun.* **1992**, *57*, 1186.
(12) Buck, U.; Ettischer, I.; Schulz, S. *Z. Phys. Chem.* **1995**, *188*, 91.
(13) Resende, S. M.; De Almeida, W. B. *Chem. Phys.* **1996**, *206*, 1.
(14) Maier, G.; Lautz, Ch. *Eur. J. Org. Chem.* **1998**, *769*, 9.
(15) Cardelino, B. H.; Moore, C. E.; Frazier, D. O.; Musaev, D. G.; Morokuma, K. *Int. J. Quantum Chem.* **1998**, *66*, 189.
(16) Karpfen, A. *J. Phys. Chem.* **1996**, *100*, 13474.
(17) Karpfen, A. *J. Phys. Chem. A* **1998**, *102*, 9286.
(18) Karpfen, A. *Mh. Chem.*, in press.
(19) Frisch, M. J.; Trucks, G. W.; Schlegel, H. B.; Gill, P. M. W.; Johnson, B. G.; Robb, M. A.; Cheeseman, J. R.; Keith, T. A.; Petersson, G. A.; Montgomery, J. A.; Raghavachari, K.; Al-Laham, M. A.; Zakrzewski, V. G.; Ortiz, J. V.; Foresman, J. B.; Cioslowski, J.; Stefanov, B. B.; Nanayakkara, A.; Challacombe, M.; Peng, C. Y.; Ayala, P. Y.; Chen, W.; Wong, M. W.; Andres, J. L.; Replogle, E. S.; Gomperts, R.; Martin, R. L.; Fox, D. J.; Binkley, J. S.; Defrees, D. J.; Baker, J.; Stewart, J. J. P.; Head-Gordon, M.; Gonzalez, C.; Pople, J. A. *Gaussian 94*, revision C.2; Gaussian, Inc.: Pittsburgh, PA, 1995.
(20) Frisch, M. J.; Trucks, G. W.; Schlegel, H. B.; Scuseria, G. E.; Robb, M. A.; Cheeseman, J. R.; Zakrzewski, J.A.; Montgomery, J. A.; Jr.; Stratmann, R. E.; Burant, J. C.; Dapprich, S.; Millam, J. M.: Daniels, A. D.; Kudin, K. N.; Strain, M. C.; Farkas, O.; Tomasi, J.; Barone, V.; Cossi, M.; Cammi, R.; Mennucci, B.; Pomelli, C.; Adamo, C.; Clifford, S.; Ochterski, J.; Petersson, G. A.; Ayala, P. Y.; Cui, Q.; Morokuma, K.; Malick, D. K.; Rabuck, A. D.; Raghavachari, K.; Foresman, J. B.; Cioslowski, J.; Ortiz, J. V.; Stefanov, B. B.; Liu, G.; Liashenko, A.; Piskorz, P.; Komaromi, I.; Gomperts, R.; Martin, R. L.; Fox, D. J.; Keith, T.; Al-Laham, M. A.; Peng, C. Y.; Nanayakkara, A.; Gonzalez, C.; Challacombe, M.; Gill, P. M. W.; Johnson, B.; Chen, W.; Wong, M. W.; Andres, J. L.; Gonzalez, C.; Head-Gordon, M.; Replogle, E. S.; and Pople, J. A. *Gaussian 98*, revision A.6; Gaussian, Inc.: Pittsburgh, PA, 1998.
(21) Møller, C.; Plesset, M. S. *Phys Rev.* **1934**, *46*, 618.
(22) Krishnan, R.; Pople, J. A. *Int. J. Quantum Chem.* **1978**, *14*, 91.
(23) Cizek, J. *Adv. Chem. Phys.* **1969**, *14*, 35.
(24) Purvis, G. D.; Bartlett, R. J. *J. Chem. Phys.* **1982**, *76*, 1910.
(25) Scuseria, G. E.; Janssen, C. L.; Schaefer, H. F., III *J. Chem. Phys.* **1988**, *89*, 7382.
(26) Scuseria, G. E.; Schaefer, H. F., III *J. Chem. Phys.* **1989**, *90*, 3700.
(27) Pople, J. A.; Head-Gordon, M.; Raghavachari, K. *J. Chem. Phys.* **1987**, *87*, 5968.
(28) Becke, A. D. *Phys. Rev.* **1988**, *A38*, 3098.
(29) Becke, A. D. *J. Chem. Phys.* **1993**, *98*, 5648.
(30) Lee, C.; Yang, W.; Parr, R. G. *Phys. Rev.* **1988**, *B37*, 785.
(31) Mielich, B.; Savin, A.; Stoll, H.; Preuss, H. *Chem. Phys. Lett.* **1989**, *157*, 200.
(32) Huzinaga, S. *J. Chem. Phys.* **1965**, *42*, 1293.
(33) Huzinaga, S. *Approximate Atomic Functions I*; University of Alberta: Edmonton, Canada, 1971.
(34) Frisch, M. J.; Pople, J. A.; Binkley, J. S. *J. Chem. Phys.* **1984**, *80*, 3265.
(35) Krishnan, R.; Binkley, J. S.; Seeger, R.; Pople, J. A. *J. Chem. Phys.* **1980**, *72*, 5639.
(36) Clark, T.; Chandrasekhar, J.; Spitznagel, G. W.; Schleyer, P. v. R. *J. Comput. Chem.* **1983**, *4*, 294.
(37) Woon, D. E.; Dunning, Th. R., Jr. *J. Chem. Phys.* **1993**, *98*, 1358.
(38) Kendall, R. E.; Dunning, Th. R., Jr.; Harrison, R. J. *J. Chem. Phys.* **1992**, *96*, 6796.
(39) Davidson, E. R. *Chem. Phys. Lett.* **1996**, *220*, 514.
(40) Boys, S. F.; Bernardi, F. *Mol. Phys.* **1970**, *19*, 553.
(41) Baldacci, A.; Ghersetti, S.; Hurlock, S. C.; Rao, K. N.; *J. Mol. Spectrosc.* **1976**, *59*, 116.
(42) Kling, H.; Geschka, H.; Huttner, W. *Chem. Phys. Lett.* **1983**, *96*, 631.
(43) Keir, R. I.; Lamb, D. W.; Ritchie, G. L. D.; Watson, J. N. *Chem. Phys. Lett.* **1997**, *279*, 22.
(44) Alms, G. R.; Burnham, A. K.; Flygare, W. H. *J. Chem. Phys.* **1975**, *63*, 3321.
(45) Strey, G.; Mills, I. M. *J. Mol. Spectrosc.* **1976**, *59*, 103.
(46) Palmer, K. F.; Mickelson, M. E.; Rao, K. N. *J. Mol. Spectrosc.* **1972**, *44*, 131.
(47) Botschwina, P. *Chem. Phys.* **1982**, *68*, 41.
(48) Lindh, R.; Liu, B. *J. Chem. Phys.* **1990**, *94*, 4356.
(49) Bone, R. G. A. *J. Phys. Chem.* **1994**, *98*, 3126.
(50) Russell, A. J.; Spackman, M. A. *Mol. Phys.* **1996**, *88*, 1109.
(51) Fowler, P. W.; Diercksen, G. H. F. *Chem. Phys. Lett.* **1990**, *167*, 105.
(52) Simandiras, E. D.; Rice, J. E.; Lee, T. J.; Amos, R. D.; Handy, N. C. *J. Chem. Phys.* **1988**, *88*, 3187.
(53) Botschwina, P. *Mol. Phys.* **1982**, *47*, 241.
(54) Matsumara, K.; Tanaka, T. *J. Mol. Spectrosc.* **1982**, *96*, 219.
(55) Maroulis, G.; Thakkar, A. J. *J. Chem. Phys.* **1991**, *95*, 9060.
(56) Williams, G. A.; Macdonald, J. M. *J. Mol. Struct.* **1994**, *320*, 217.
(57) Owen, N. L.; Smith, Ch. H.; Williams, G. A. *J. Mol. Struct.* **1987**, *161*, 33.
(58) McNaughton, D.; Bruget, D. N. *J. Mol. Struct.* **1992**, *273*, 11.
(59) Jaffe, R. L.; Smith, G. D. *J. Chem. Phys.* **1996**, *105*, 2780.
(60) Hobza, P.; Selzle, H. L.; Schlag, E. W. *J. Phys. Chem.* **1996**, *100*, 18790.
(61) Sponer, J.; Hobza, P. *Chem. Phys. Lett.* **1997**, *267*, 263.